Απεικόνιση Δορυφόρων

Γεώργιος Κ. Παπανικολάου
Stanford University
papanicolaou@stanford.edu
http://virtualmath1.stanford.edu/~papanico

Εθνικό Μετσόβιο Πολυτεχνείο

18 Δεκεμβρίου 2019

Οι συνεργάτες μου στην απεικόνιση δορυφόρων

- L. Borcea (U. Michigan)
- J. Fournier (Ecole Normale Paris)
- J. Garnier (Ecole Polytechnique)
- M. Leibovich (Stanford)
- Χ. Τσόγκα (Παν. Κρήτης, U.C. Merced)
- K. Solna (U.C. Irvine)

Outline of presentation

- Brief review of low earth orbit satellites and why do satellite imaging research now
- Imaging schematic and quick derivation of a formula for the signal recorded by receivers in satellite imaging (mathematical)
- The imaging algorithms: Matched Field (MF), in common use today, and Cross Correlation (CC) Imaging, proposed
- Resolution limits
- What is ahead in this research

Sixty two years into the space age

- On October 4 1957 the first man-made satellite went into orbit: A spherical object of diameter 58 cm at an average altitude of about 500 km, and cycling the earth with a period of 96 minutes.
- In Low Earth Orbit (LEO), 200-1500 km, there are some 10,000 objects that are being tracked today.
- At higher altitudes , the geosynchronous orbit, which is about 5 earth radii from the earth's surface (about 35,000 km), there are some 20,000 objects large enough to be tracked (more than 50 cm diameter).
- At an altitude of 500 km a satellite is traveling at a speed of 7.6 km per second (more than 27,000 km per hour) so as to stay in orbit.

Man-made space debris

- More than 170 million pieces of debris of size one centimeter and smaller.
- They descend in altitude slowly because of drag, on the scale of decades, especially the ones at higher altitude where there is less drag.
- These small objects are fragments from disintegrating larger satellites. They can come from collisions, from booster rockets, etc.
- They fly at speeds three to four times faster than bullets from high-performance guns.
- When collisions occur in space they generate a lot of debris that disperses widely.

Space debris science forty years ago

VOL. 83, NO. A6 JOURNAL OF GEOPHYSICAL RESEARCH JUNE 1, 1978

Collision Frequency of Artificial Satellites: The Creation of a Debris Belt

DONALD J. KESSLER AND BURTON G. COUR-PALAIS

NASA Johnson Space Center, Houston, Texas 77058

As the number of artificial satellites in earth orbit increases, the probability of collisions between satellites also increases. Satellite collisions would produce orbiting fragments, each of which would increase the probability of further collisions, leading to the growth of a belt of debris around the earth. This process parallels certain theories concerning the growth of the asteroid belt. The debris flux in such an earth-orbiting belt could exceed the natural meteoroid flux, affecting future spacecraft designs. A mathematical model was used to predict the rate at which such a belt might form. Under certain conditions the belt could begin to form within this century and could be a significant problem during the next century. The possibility that numerous unobserved fragments already exist from spacecraft explosions would decrease this time interval. However, early implementation of specialized launch constraints and operational procedures could significantly delay the formation of the belt.

Notable early research on space debris

Debris distribution today

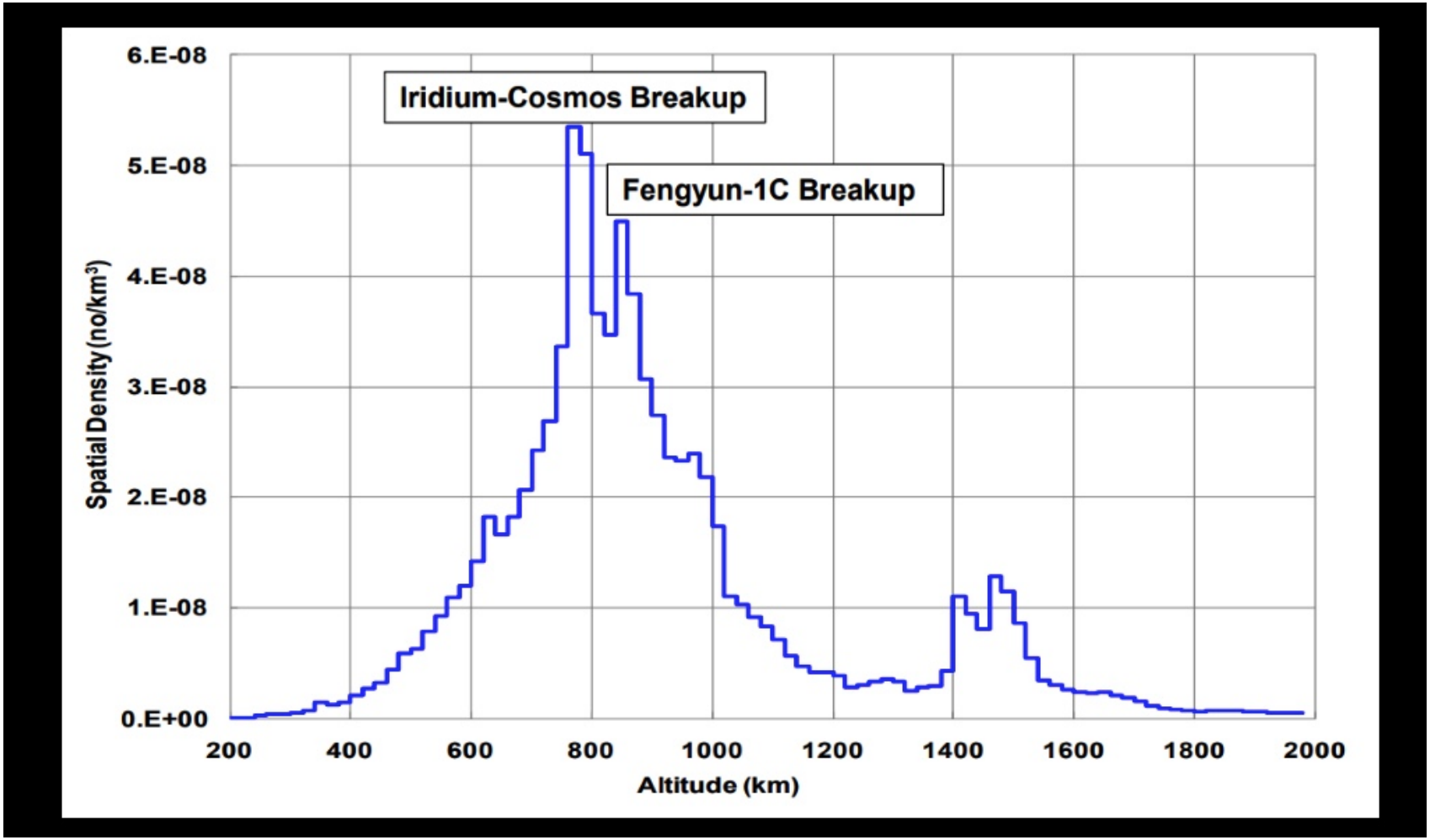

Estimated radial debris distribution

Notable "collisions" in space

- China in 2007 carried out an anti-missile test in space (800 km) that generated the largest amount of debris in history. It was immediately criticized internationally, and it probably surprised China that debris is indeed an issue of serious concern.
- In 2008 the US destroyed a defective satellite that was believed to cary toxic material. It was at an altitude of 250 km. Most of the debris that was generated had dissipated into the atmosphere below by 2009.
- At around 2009 the US government became very concerned about the lack of adequate space surveillance capabilities, especially for emergencies.

Government and private enterprise in space

- Until about 2014 most of the activity in space was carried out by the government, mostly the military and NASA. An exception are the geosynchronous satellites (about 600), for communications and weather forecasting.
- Privately owned and operated satellite constellations (some 1000 small satellites) begun to appear in the last 5 years in order to provide large-scale and repeated remote sensing services.
- Applications: Agriculture, livestock, real estate, forestry, coastline erosion, shifting climate patterns, urban planning, ...
- On demand satellite remote sensing services: A new industry ... and a challenge

But there is RISK

- How do you insure an investment of many millions for a satellite constellation in space?
- How do you check that the constellation is in normal condition?
- Who provides LEO surveillance services on demand? Only one company at this time.
- There are huge obstacles in providing reliable and accurate on-demand LEO surveillance. Most difficult one: High-power ground-based radar illumination. Very expensive, now entirely controlled by governments, not flexible, ...

Need inexpensive and efficient space surveillance

Once government funding is gone then cost and efficiency matter and must be calculated carefully.

It is all about tools for risk assessment. And perhaps most important is space surveillance tools that provide diverse information.

What we propose

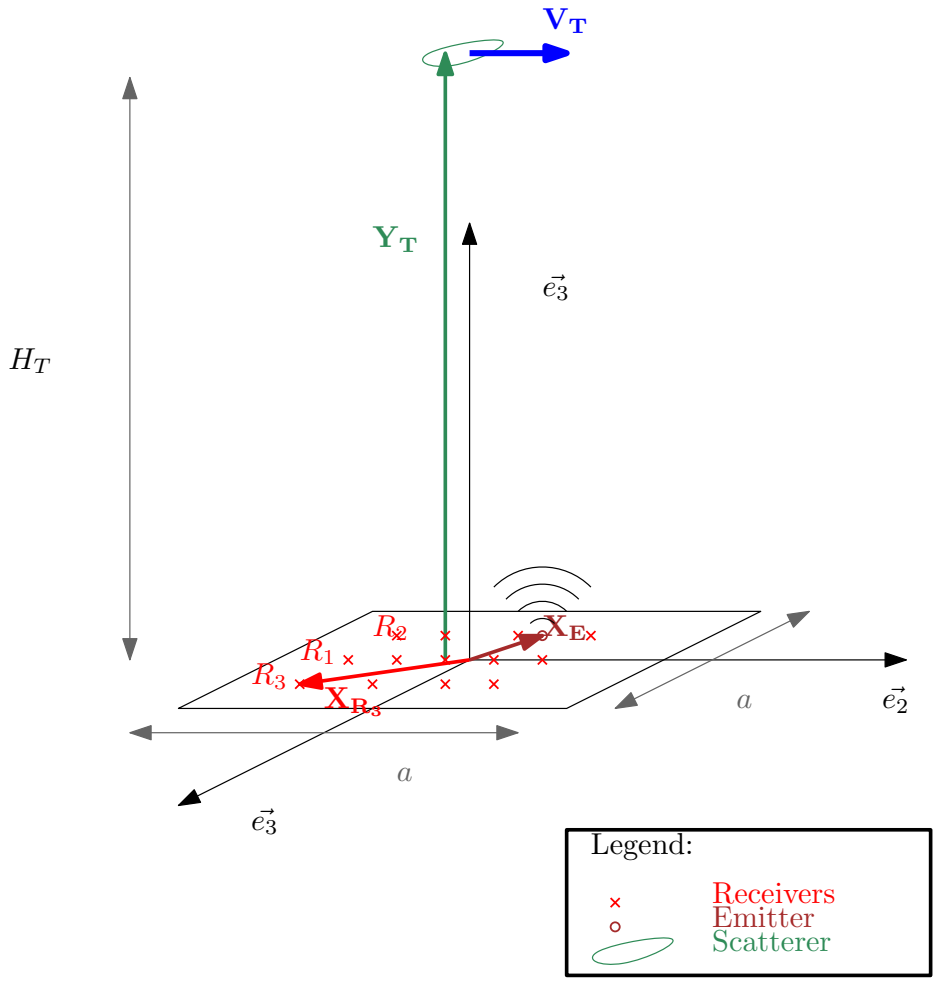

Schematic of drone-based receivers, asynchronous and distributed ground-based radar illumination, and the use of correlation-based imaging (Garnier-Papanicolaou, CUP 2016, and FGPT, SIIMS 2017).

How did this research project start

Use of passive sensor arrays as a way to image (a) through strongly inhomogeneous media, and (b) with independent, asynchronous, and unknown (often opportunistic) illumination.

1. Started in seismic imaging for hydrocarbons around 2005 but has a longer history. Around 2010 passive synthetic aperture radar (SAR) begun to be used for imaging ground reflectivities using opportunistic illumination, either ground based or from satellites[1].
2. We decided to consider passive SAR to image satellites. The passive recording platform(s) is (are) to fly above the atmosphere (at about 20 km or more), the illumination coming from the ground. The satellite is in low earth orbit (at about 300-1200 km), and is rapidly moving (to remain in orbit).

[1] Passive Imaging with Ambient Noise, Garnier and Papanicolaou, Cambridge University Press 2016

Theory and numerical simulations show that:

1. The effect of atmospheric inhomogeneities is reduced with high-flying, passive receivers (Garnier+P, SIIMS 2014 and 2015).
2. Can have good resolution analysis. (Analytically challenging but can be done from first principles. Key: create an effective hierarchy of approximations)
3. Ground-based matched-filter imaging (currently in use) and (the proposed) passive receiver, correlation-based imaging can be compared.
4. Main result: In the X-Band (10 GHz) regime, and with six to nine recording platforms (ground-based or drones) over a 200×200 kilometer region the satellite position and velocity image resolutions are comparable for the two modalities, can be quantified very well, and are close to optimal, down to centimeter level (with a wavelength of 3cm).

Scaterring by a moving object

A (point) transmitter at $\boldsymbol{X}_{\mathrm{E}}$ emits a short pulse $\mathrm{f}(\mathrm{t})$. The total field $\mathfrak{u}(\mathrm{t}, \boldsymbol{x})$ solves

$$\frac{1}{\mathrm{c}^2(\mathrm{t}, \boldsymbol{x})} \frac{\partial^2 \mathfrak{u}}{\partial \mathrm{t}^2} - \Delta \mathfrak{u} = \mathrm{f}(\mathrm{t}) \delta(\boldsymbol{x} - \boldsymbol{X}_{\mathrm{E}}), \tag{1}$$

with a localized perturbation ρ_{T} centered at the moving target $\boldsymbol{X}_{\mathrm{T}}(\mathrm{t})$,

$$\frac{1}{\mathrm{c}^2(\mathrm{t}, \boldsymbol{x})} = \frac{1}{\mathrm{c}_{\mathrm{o}}^2} \Big(1 + \rho_{\mathrm{T}} \big(\boldsymbol{x} - \boldsymbol{X}_{\mathrm{T}}(\mathrm{t}) \big) \Big).$$

The incident field $\mathfrak{u}^{(0)}(\mathrm{t}, \boldsymbol{x})$ is

$$\mathfrak{u}^{(0)}(\mathrm{t}, \boldsymbol{x}) = \frac{1}{4\pi |\boldsymbol{x} - \boldsymbol{X}_{\mathrm{E}}|} \mathrm{f}\Big(\mathrm{t} - \frac{|\boldsymbol{x} - \boldsymbol{X}_{\mathrm{E}}|}{\mathrm{c}_{\mathrm{o}}} \Big). \tag{2}$$

The scattered field

In the Born approximation the scattered field is given by

$$u^{(1)}(t,\boldsymbol{x}) = -\frac{1}{c_o^2}\int_0^t d\tau \int d\boldsymbol{y} G(t-\tau,\boldsymbol{x},\boldsymbol{y})\rho_T(\boldsymbol{y}-\boldsymbol{X}_T(\tau))\frac{\partial^2}{\partial\tau^2}u^{(0)}(\tau,\boldsymbol{y}).$$

For a point-like scatterer,

$$u^{(1)}(t,\boldsymbol{x}) = -\frac{\rho}{c_o^2}\int_0^t d\tau G(t-\tau,\boldsymbol{x},\boldsymbol{X}_T(\tau))\frac{\partial^2}{\partial\tau^2}u^{(0)}(\tau,\boldsymbol{y})\mid_{\boldsymbol{y}=\boldsymbol{X}_T(\tau)},$$

where $\rho = \int \rho_T(\boldsymbol{x})d\boldsymbol{x}$ is the reflectivity of the target. Using $u^{(0)}$ and integrating by parts twice:

$$u^{(1)}(t,\boldsymbol{x}) = -\frac{\rho}{c_o^2}\int_0^t d\tau \int_0^\tau d\tau' f''(\tau') G(\tau-\tau',\boldsymbol{X}_T(\tau),\boldsymbol{X}_E) G(t-\tau,\boldsymbol{x},\boldsymbol{X}_T(\tau)).$$

Therefore the scattered field at the receiver at $\boldsymbol{x} = \boldsymbol{X}_R$ is

$$\begin{aligned} u_{s,R}(t) &= -\frac{\rho}{c_o^2}\int_0^t d\tau \frac{1}{4\pi|\boldsymbol{X}_T(\tau)-\boldsymbol{X}_E|} f''\Big(\tau - \frac{|\boldsymbol{X}_T(\tau)-\boldsymbol{X}_E|}{c_o}\Big) \\ &\quad \times \frac{1}{4\pi|\boldsymbol{X}_R-\boldsymbol{X}_T(\tau)|}\delta\Big(t-\tau-\frac{|\boldsymbol{X}_R-\boldsymbol{X}_T(\tau)|}{c_o}\Big). \end{aligned}$$

The scattered field, continued

If we introduce

$$\Phi(\tau; t) = t - \tau - \frac{|\boldsymbol{Y}_T - \boldsymbol{X}_R + \tau \boldsymbol{V}_T|}{c_o},$$

then we have

$$\delta\left[\Phi(\tau; t)\right] = \frac{\delta[\tau - \tau(t)]}{|\partial_\tau \Phi(\tau(t); t)|},$$

with $\tau(t)$ the unique zero of $\tau \to \Phi(\tau; t)$ in $(0, t)$. Denoting $\boldsymbol{D}(t) = \boldsymbol{Y}_T - \boldsymbol{X}_R + t\boldsymbol{V}_T$, We find that $\tau(t)$ is given by

$$\tau(t) = t - \frac{|\boldsymbol{D}(t)|}{c_o\left(1 - \left|\frac{\boldsymbol{V}_T}{c_o}\right|^2\right)} \left[\sqrt{1 - \left|\frac{\boldsymbol{V}_T}{c_o}\right|^2 + \left(\frac{\boldsymbol{V}_T}{c_o} \cdot \frac{\boldsymbol{D}(t)}{|\boldsymbol{D}(t)|}\right)^2} - \frac{\boldsymbol{V}_T}{c_o} \cdot \frac{\boldsymbol{D}(t)}{|\boldsymbol{D}(t)|}\right]. \tag{3}$$

Using this in $u_{s,R}(t)$ we get the (model) signal recorded at the receiver

$$u_{s,R}(t) = -\frac{\rho f''\left(\tau(t) - \frac{|\boldsymbol{X}_T(\tau(t)) - \boldsymbol{X}_E|}{c_o}\right)}{(4\pi)^2 c_o^2 |\boldsymbol{X}_T(\tau(t)) - \boldsymbol{X}_E||\boldsymbol{X}_R - \boldsymbol{X}_T(\tau(t))| \left|1 + \frac{\boldsymbol{V}_T}{c_o} \cdot \frac{\boldsymbol{D}(\tau(t))}{|\boldsymbol{D}(\tau(t))|}\right|}. \tag{4}$$

What is the imaging problem

- We record signals $u_{s,R}(t)$ at various receiver locations $\boldsymbol{X}_R$. These locations (not moving for simplicity here) are assumed known.
- The source location $\boldsymbol{X}_E$ must be know in matched field imaging.
- The source(s) need only be known roughly for correlation based imaging, and there may be several sources. Asynchronous illumination can be very effective.
- We want to find (estimate) the target location $\boldsymbol{Y}_T$ and velocity $\boldsymbol{V}_T/c_o$ assumed to be small. This is a point in six dimensions in general. For satellites in orbit it can be reduced to five with a "tangential" $\boldsymbol{V}_T$.

How are we to do this? We construct Imaging functions.

Imaging functions: Matched field

The idea behind the matched-filter imaging function is that we want to match the received signal with the emitted pulse. The matching process involves the assumed initial position and speed of the object $(\boldsymbol{Y}, \boldsymbol{V})$, and this matching can be shown to be maximal at the true position $(\boldsymbol{Y}_{\mathrm{T}}, \boldsymbol{V}_{\mathrm{T}})$. The matching process takes into account a (derived) Doppler compensation factor $\gamma_{\mathrm{s}}(\boldsymbol{X}, \boldsymbol{V}, \boldsymbol{X}_{\mathrm{R}})$,

$$\mathcal{I}^{\mathrm{MF}}(\boldsymbol{Y}, \boldsymbol{V}) = \frac{1}{\mathrm{N_E}} \sum_{\mathrm{j}=1}^{\mathrm{N_E}} \mathcal{I}_{\mathrm{j}}^{\mathrm{MF}}(\boldsymbol{Y} + \boldsymbol{V}\mathrm{S_j}, \boldsymbol{V}),$$

$$\mathcal{I}_{\mathrm{j}}^{\mathrm{MF}}(\boldsymbol{X}, \boldsymbol{V}) = \frac{1}{\mathrm{N}} \sum_{\mathrm{R}=1}^{\mathrm{N}} \int \mathrm{f}\Big(\gamma_{\mathrm{s}}(\boldsymbol{X}, \boldsymbol{V}, \boldsymbol{X}_{\mathrm{R}})\big(\mathrm{t} - \frac{|\boldsymbol{X} - \boldsymbol{X}_{\mathrm{R}}|}{\mathrm{c_o}}\big) - \frac{|\boldsymbol{X} - \boldsymbol{X}_{\mathrm{E}}|}{\mathrm{c_o}}\Big) \mathrm{u}_{\mathrm{s,R}}(\mathrm{S_j} + \mathrm{t})\mathrm{dt}$$

This imaging function requires knowledge of the transmitter and receiver positions $\boldsymbol{X}_{\mathrm{E}}$ and $\boldsymbol{X}_{\mathrm{R}}$. We also need to know the pulse profile f. One wants to image a region around some point $\boldsymbol{Y}_{\mathrm{T}}$, so the j-th scattered signal needs only to be recorded for a short time around $2|\boldsymbol{Y}_{\mathrm{T}} - \boldsymbol{X}_{\mathrm{E}}|/\mathrm{c_o}$.

Imaging functions: Cross correlations

We cross correlate the scattered signals recorded by pairs of receivers and migrate them with the appropriate Doppler compensation factors,

$$\mathcal{I}^{CC}(\boldsymbol{Y},\boldsymbol{V}) = \frac{1}{N_E}\sum_{j=1}^{N_E}\mathcal{I}_j^{CC}(\boldsymbol{Y}+\boldsymbol{V}S_j,\boldsymbol{V}), \tag{5}$$

$$\mathcal{I}_j^{CC}(\boldsymbol{X},\boldsymbol{V}) = \frac{1}{N^2}\sum_{R,R'=1}^{N}\int u_{s,R}\left(S_j+\frac{|\boldsymbol{X}-\boldsymbol{X}_R|}{c_o}+\frac{t+\frac{|\boldsymbol{X}-\boldsymbol{X}_E|}{c_o}}{\gamma_s(\boldsymbol{X},\boldsymbol{V},\boldsymbol{X}_R)}\right)$$
$$\times u_{s,R'}\left(S_j+\frac{|\boldsymbol{X}-\boldsymbol{X}_{R'}|}{c_o}+\frac{t+\frac{|\boldsymbol{X}-\boldsymbol{X}_E|}{c_o}}{\gamma_s(\boldsymbol{X},\boldsymbol{V},\boldsymbol{X}_{R'})}\right)dt. \tag{6}$$

Now it is not necessary to know the pulse profile f, which could be different from one emission to another one. It is not necessary either to know the emission times with accuracy. But we need to record the whole train of scattered signals. Moreover correlation-based imaging has been shown to be robust to medium fluctuations when in a suitable imaging configuration[2].

[2] Garnier+P, CUP, 2016

Simplified setup for the simulations

- We assume that there is a single illuminating source on the ground, whose location need not be known for CC imaging. The emitted signals (synchronization, pulse form) are also not known. They are, however assumed known for MF imaging.
- The 6-9 recording platforms are stationary (as their motion makes little difference in resolution if assumed known) and randomly placed in a 200×200 kilometer square at a fixed altitude. The satellite flies in the Y_2 direction (into the screen) at constant speed starting right above the source on the ground.
- With only about 6-9 recording platforms we get as good a resolution as if we had a full 200×200 kilometer aperture. Both with CC and MF imaging.

Satellite imaging with (passive) X-band SAR

System Parameters		
Central Frequency	f_0	9.6 GHz
Bandwidth	B	622 MHz
Number of Frequencies in Bandwidth	N_f	515
Slow-time Sampling	Δs	0.015 s
Wave Speed	c_o	3×10^8 m/s
Central Wavelength	λ_o	3.12 cm
Altitude of Satellite	H	500 km
Speed of Satellite	V_T	7,610.6 m/s
Altitude of Drone	h	20 km
Velocity of Drone	V_R	222.2 m/s (800 km/hr)

Parameters for modeling SAR imagining of a satellite with passive SAR on a platform above the atmosphere and microwave sources on the ground.

Resolution results from the simulation

- There are five "parameters" to be imaged: The three components of the satellite (say its initial) location and the (assumed) two components of its speed. We actually include vertical speed as well since it is needed when dealing with larger size space objects.
- The passive SAR platform covers a distance of 5 km, in 22.5 secs. During this time the satellite covers a distance of 171 km. These are the recording windows used.

MF theoretical imaging resolution formulas obtained

		X-band	**S-band**
Y_1	$\frac{\lambda_o H_T}{a}$	3.75 cm	18.75 cm
Y_2	$\lambda_o(\frac{H_T}{a} \wedge \frac{H_T}{2V_T T_{tot}})$	3.75 cm $\wedge$4.4 cm $=$ 3.75 cm	18.75 cm
Y_3	$\frac{c_o}{2B} \wedge \lambda_o \frac{H_T^2}{2V_T T_{tot} a}$	23 cm $\wedge$5.5 cm $=$ 5.5 cm	27.5 cm
V_1	$\frac{\lambda_o H_T}{a T_{tot}}$	0.17 cm/s	0.85 cm/s
V_2	$\frac{\lambda_o}{T_{tot}}(\frac{H_T}{a} \wedge \frac{H_T}{2V_T T_{tot}})$	0.17 cm/s $\wedge$0.19 cm/s $=$ 0.17 cm/s	0.85 cm/s
V_3	$\frac{\lambda_o}{2T_{tot}}$	0.07 cm/s	0.35 cm/s

CC theoretical imaging resolution formulas obtained

		X-band	**S-band**
$\boldsymbol{Y}_{\perp}$	$\frac{\lambda_o H_T}{a}$	3.75 cm	18.75 cm
Y_3	$\lambda_o\left(\frac{H_T^2}{a^2} \wedge \frac{2H_T^2}{aV_T T_{tot}}\right)$	4.7 cm $\wedge$22 cm $=$ 4.7 cm	23.5 cm
$\boldsymbol{V}_{\perp}$	$\frac{\lambda_o H_T}{aT_{tot}}$	0.17 cm/s	0.85 cm/s
V_3	$\frac{\lambda_o}{T_{tot}}\left(\frac{H_T^2}{a^2} \wedge \frac{2H_T^2}{aV_T T_{tot}}\right)$	0.2 cm/s $\wedge$1 cm/s $=$ 0.2 cm/s	1 cm/s

MF and CC horizontal-horizontal (Y_1, Y_2) resolutions

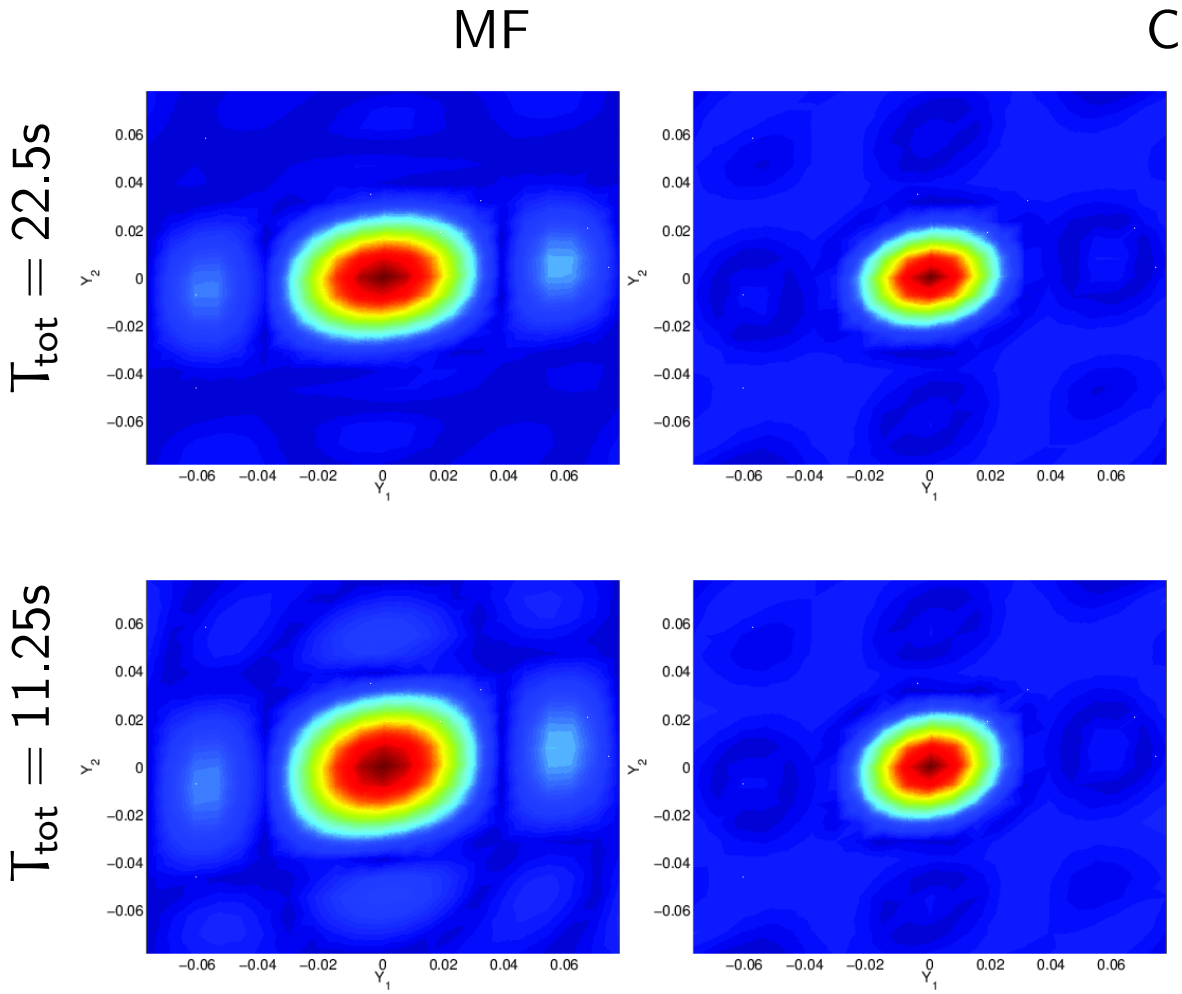

Images with MF and CC in the (Y_1, Y_2) plane. The units are in m. The satellite velocity is $V_T = 7610$m/s. The first row is for recording duration $T_{tot} = 11.25$s and the second for $T_{tot} = 22.5$s.

MF and CC horizontal-vertical (Y_1, Y_3) resolutions

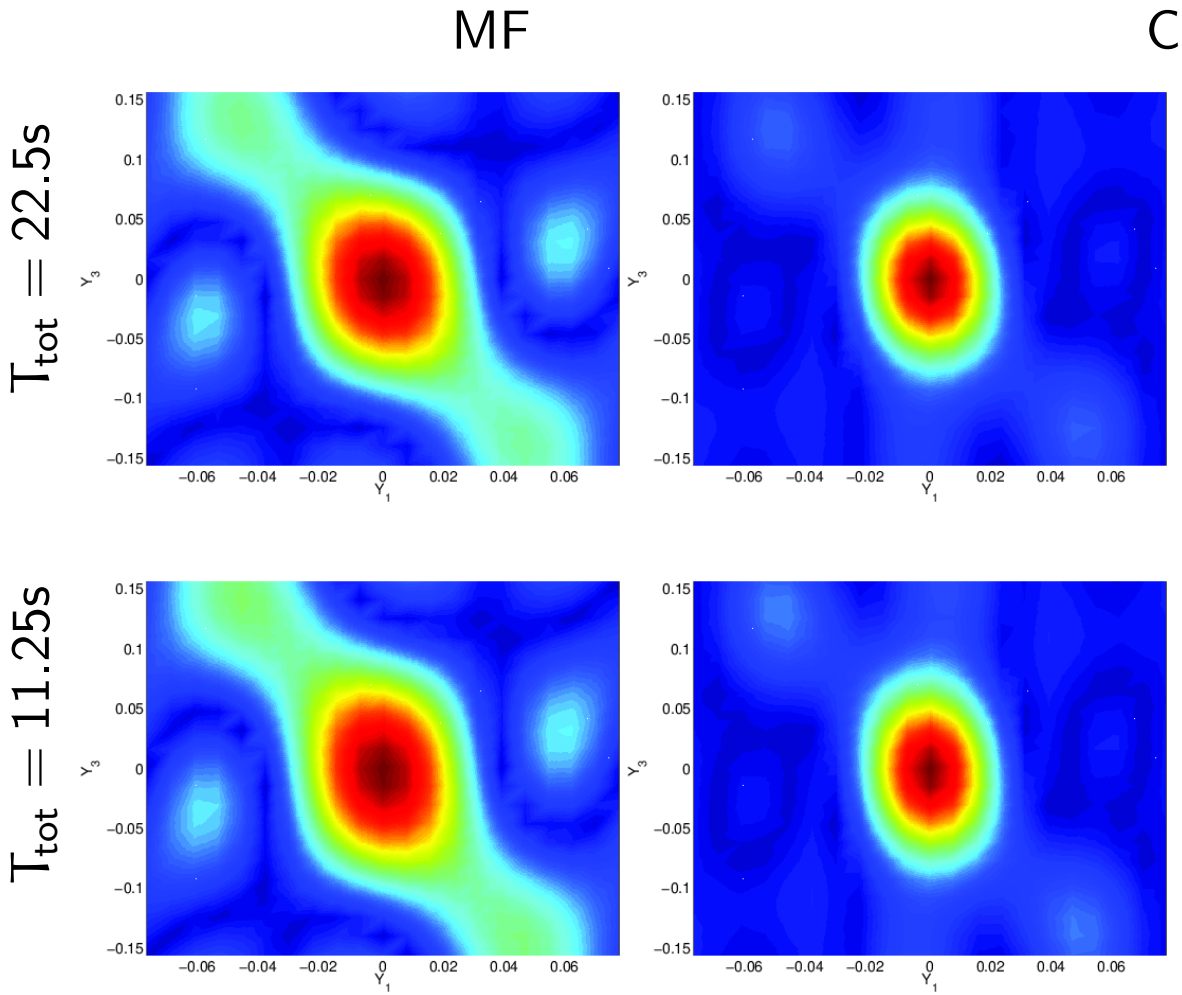

Images with MF and CC in the plane (Y_1, Y_3). The units are in m. The satellite velocity is $V_T = 7610$m/s. The first row is for recording duration $T_{tot} = 11.25$s and the second for $T_{tot} = 22.5$s.

MF and CC horizontal-horizontal (V_1, V_2) velocity resolutions

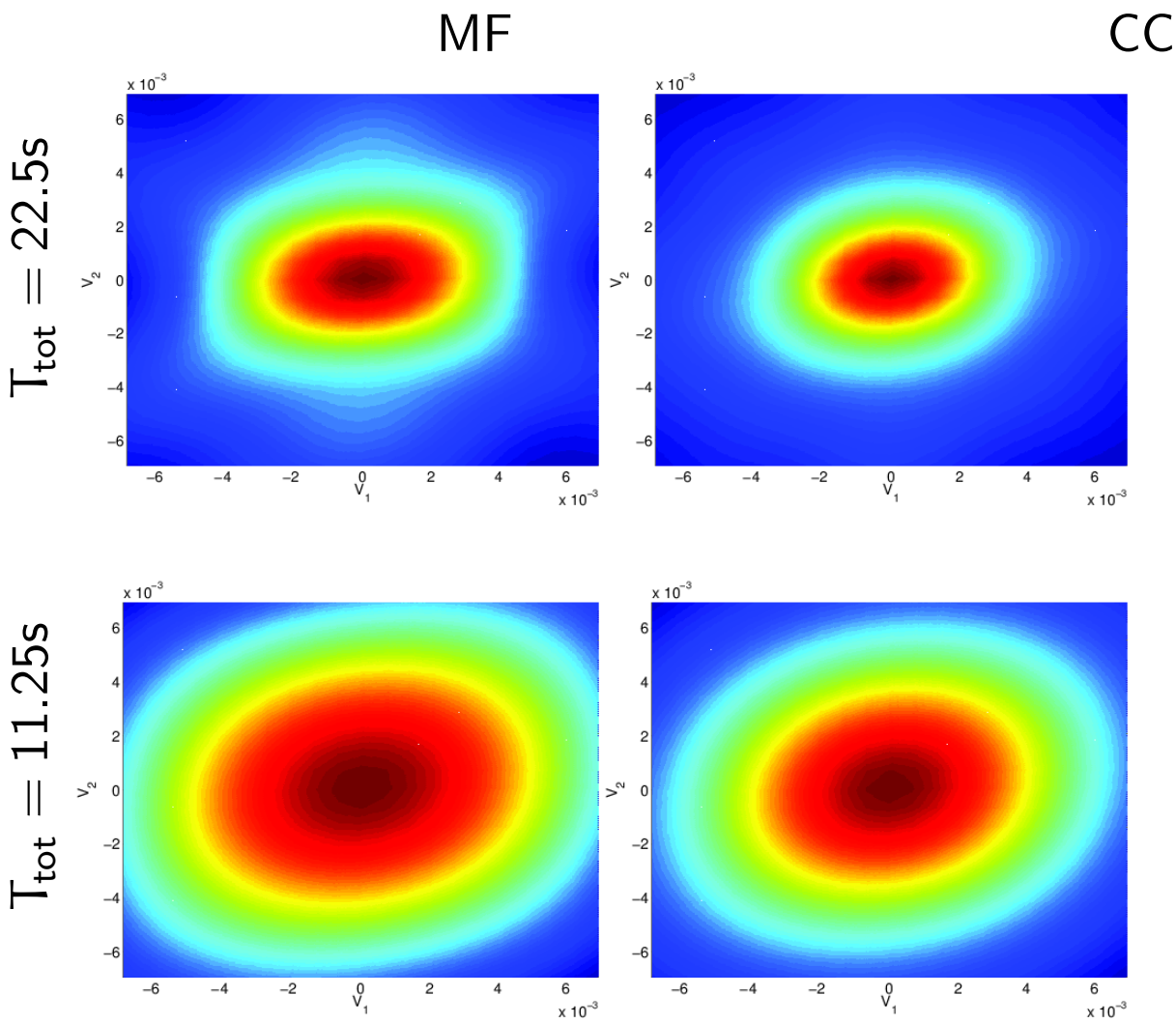

The abscissa is for V_1 and the ordinate for V_2. The units are in m/s. The

MF and CC horizontal-vertical (V_1, V_3) velocity resolution

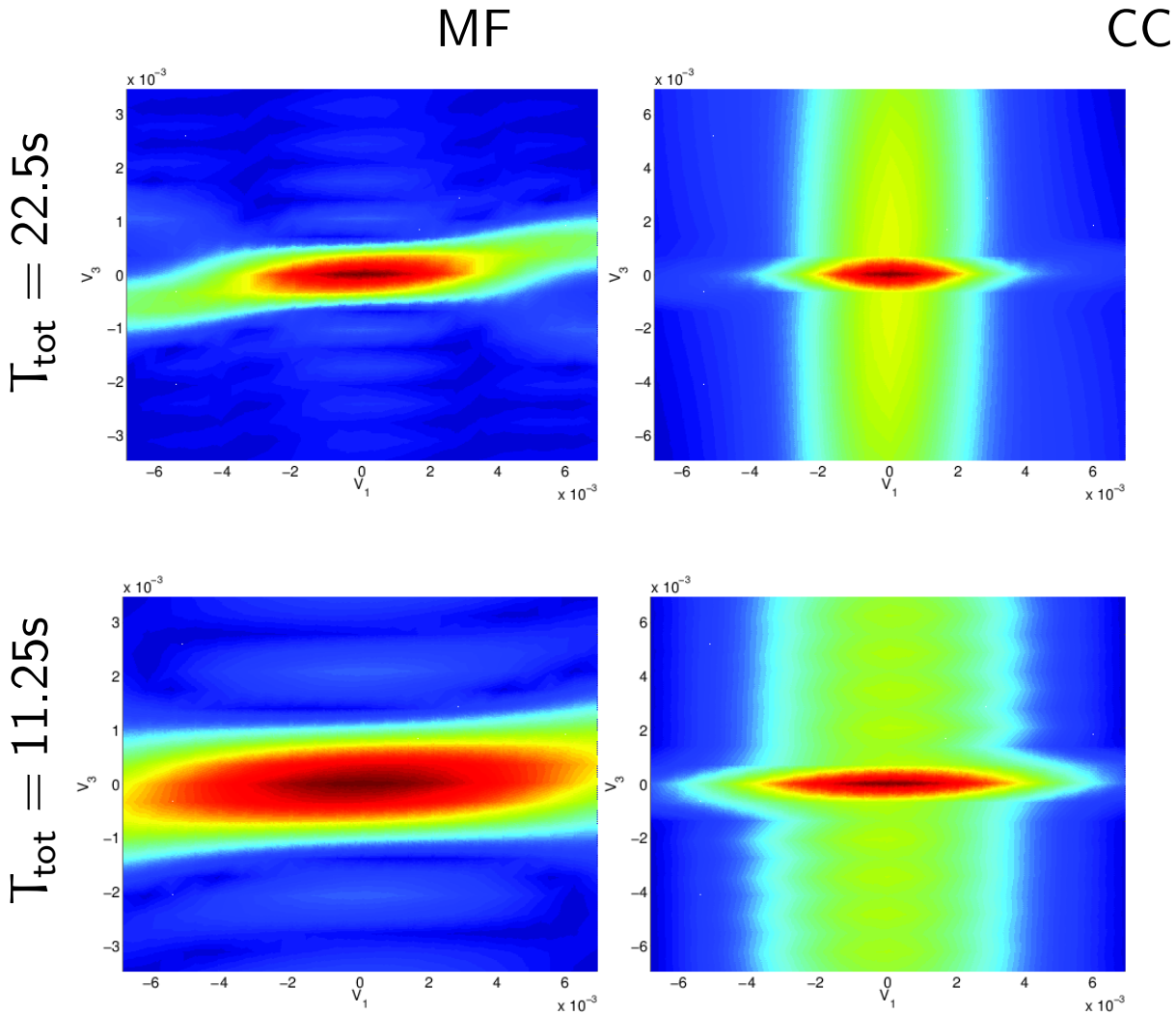

The abscissa is for V_1 and the ordinate for V_3. The units are in m/s. The satellite velocity is $V_T = 7610$m/s. The first row is for recording duration $T_{tot} = 11.25$s and the second for $T_{tot} = 22.5$s.

Summary

- We have shown that passive SAR imaging of satellites can be done with a resolution that is essentially the optimal one, properly interpreted, when using a suitably adjusted imaging function to account for rapid target motion. The resolution theory is challenging but essentially complete now, both for CC and MF (currently used) imaging. CC and MF imaging resolutions are comparable for multiple receivers (continuum approximation) and "large" apertures[3].
- CC imaging is robust to atmospheric inhomogeneities when for example the satellite is low in the horizon and signal paths are long inside the atmosphere. Numerical simulations to explore this need to be done and are challenging.
- Need to address: Synchronization issues, SNR issues, finite size satellite effects, including rotation, swarms of debris, global small scale tracking .... Sparse Arrays ...

[3] Two papers in the SIAM J. on Imaging Science, 2017

What are the objectives in the next year or two?

- Study the limits of low power ground-based illumination
- Study the effects of the atmosphere in satellite imaging, especially at higher frequencies (W-band, 3 mm wavelength).
- Study the possibility of imaging simultaneously and in detail large clusters of debris.